

## Spectroscopic study on the intermolecular interaction of SO<sub>2</sub> absorption in poly-ethylene glycol+H<sub>2</sub>O systems

Zhiqiang He, Jinrong Liu<sup>†</sup>, Jianbin Zhang<sup>†</sup>, and Na Zhang

College of Chemical Engineering, Inner Mongolia University of Technology, Huhhot 010051, China

(Received 27 August 2013 • accepted 21 November 2013)

**Abstract**—Poly-Ethylene Glycol (PEG) 300+H<sub>2</sub>O solutions (PEGWs) has been used as a promising medium for the absorption of SO<sub>2</sub>. We investigated the UV, FTIR, <sup>1</sup>H-NMR, and fluorescence spectra in the absorption processes of SO<sub>2</sub> in PEGWs to present an important absorption mechanism. Based on the spectral results, the possibility of intermolecular hydrogen bond formation by hydroxyl oxygen atom in the PEG molecule with hydrogen atom in H<sub>2</sub>O and S···O interaction formation by the oxygen atoms in PEG with the sulfur atom in SO<sub>2</sub> are discussed. This shows that the spectral changes may be due to the formation of -CH<sub>2</sub>CH<sub>2</sub>O(H)···HOH··· and -CH<sub>2</sub>-CH<sub>2</sub>-O(CH<sub>2</sub>-CH<sub>2</sub>)···HOH··· in PEGWs and the formation of -CH<sub>2</sub>CH<sub>2</sub>OH···OSO···, and intermolecular S···O interaction between PEG and SO<sub>2</sub> as the formation of -CH<sub>2</sub>CH<sub>2</sub>OCH<sub>2</sub>CH<sub>2</sub>O(H)···(O)S(O)··· and -CH<sub>2</sub>-CH<sub>2</sub>-O(CH<sub>2</sub>-CH<sub>2</sub>)···(O)S(O)···. The existence of these bonds benefits the absorption and desorption processes of SO<sub>2</sub> in PEGWs.

Keywords: Poly-ethylene Glycol (PEG) 300, Sulfur Dioxide, Absorption, Hydrogen Bonding, S···O Interaction

### INTRODUCTION

Sulfur dioxide (SO<sub>2</sub>), which is emitted from power plants and industrial plants, is a significant source gas of atmospheric pollution that threatens the environment and human health [1]. It needs to be removed from flue gases before it is released. Many technologies for removing SO<sub>2</sub> have been proposed, of which the conventional procedures, such as limestone scrubbing [2-4] and ammonia scrubbing, have some inherent disadvantages, including high capital and operating costs, a larger water requirement, poor quality of byproduct, and secondary pollution [5,6]. Because of the favorable absorption and desorption properties for acid gases in industrial processes, organic solvents have become the subject of increasing interest in recent years [7-9]. Wei, Zhang and their co-workers have paid great attention to the alcohol system to remove SO<sub>2</sub> for several years [10-18].

Poly-ethylene glycol (PEG) 300, an important industrial solvent, has been used in the absorption study of SO<sub>2</sub> for its low toxicity, low vapor pressure, and low melting point. Both PEG and its aqueous solutions (PEGWs) indicate that the strong solubility of SO<sub>2</sub> may be related to hydrogen bonding and interaction between PEG and SO<sub>2</sub>. This work is a continuous study based on the previous investigations, such as density, viscosities, excess molar volumes [19] and solubility of SO<sub>2</sub> in PEGWs [20], and the spectroscopic study can provide an important absorption mechanism for the design and operation of PEGWs in further industrial desulfurization application.

For the researches of the SO<sub>2</sub> absorption mechanism in PEGW, FTIR, UV, and fluorescence spectroscopy are used to probe the intermolecular hydrogen bonding [21,22] and interaction among molecules, since FTIR spectroscopy presents precise information about

water-sensitive bonds [23,24] and the PEG characteristic vibrational properties. Furthermore, FTIR is also advantageous for evaluating vibrational properties of bonds through very thin solution films, which are usually difficult to handle for the floating properties of solution. UV and fluorescence spectroscopy give important information about various electronic transitions. Generally, FTIR [25,26], UV, and fluorescence spectroscopy offer the advantages of measuring the association properties and hydrogen bonding capability, and assessing the interaction of alcohol with water by analyzing band shifts and changes.

The present work mainly focuses on spectral investigation, which is part of the continuation of this ongoing study on the solubility properties, because knowledge about the absorption mechanism is another important feature in industrial natural gas treating processes except for the basic physicochemical properties published before

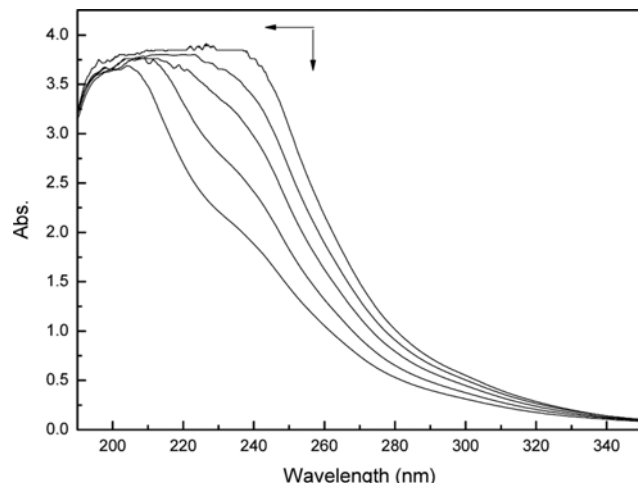


**Fig. 1.** UV spectral changes of PEGW at various mass fractions with increasing H<sub>2</sub>O concentration.

<sup>†</sup>To whom correspondence should be addressed.

E-mail: liujr@imut.edu.cn, tadzhang@pku.edu.cn

Copyright by The Korean Institute of Chemical Engineers.

[19,20]. Our results provide an important molecular mechanism for the design and operation of the absorption and desorption process in flue gas desulfurization (FGD) with potential industrial application of various PEGWs.

## EXPERIMENTAL

The analytical grade PEG with a purity of 99% (mass fraction) was purchased from Beijing Reagent Company (China), which was used after drying over molecular sieves (type 4A) and oscillation degassing. The purity of PEG was checked in the previous work [19]. The SO<sub>2</sub> gas (99.9%) and the certified standard mixture (SO<sub>2</sub>+

N<sub>2</sub>, y<sub>SO<sub>2</sub></sub>=5·10<sup>-4</sup>) were purchased from the Beijing Oxygen Plant Specialty Gases Institute Company. All the gases were decompressed and filtered before measurements. Double-distilled water was used, and the mixture solutions were prepared by mass using an analytical balance (Sartorius BS224S) with a precision of ±0.0001 g.

UV-vis spectra were recorded on a Varian CARY 1E UV-vis spectrometer in the range of (190 to 900) nm. Fluorescence spectra were acquired using an F-4500 fluorescence spectrophotometer employing a 500 W Hg-Xe high pressure lamp. FTIR spectra were recorded on a Bruker VECTOR22 FTIR spectrometer with a resolution of 1 cm<sup>-1</sup> at 298 K in the range from 4,000 cm<sup>-1</sup> to 400 cm<sup>-1</sup>. The spectrometer possesses auto-align energy optimization and a dynamical

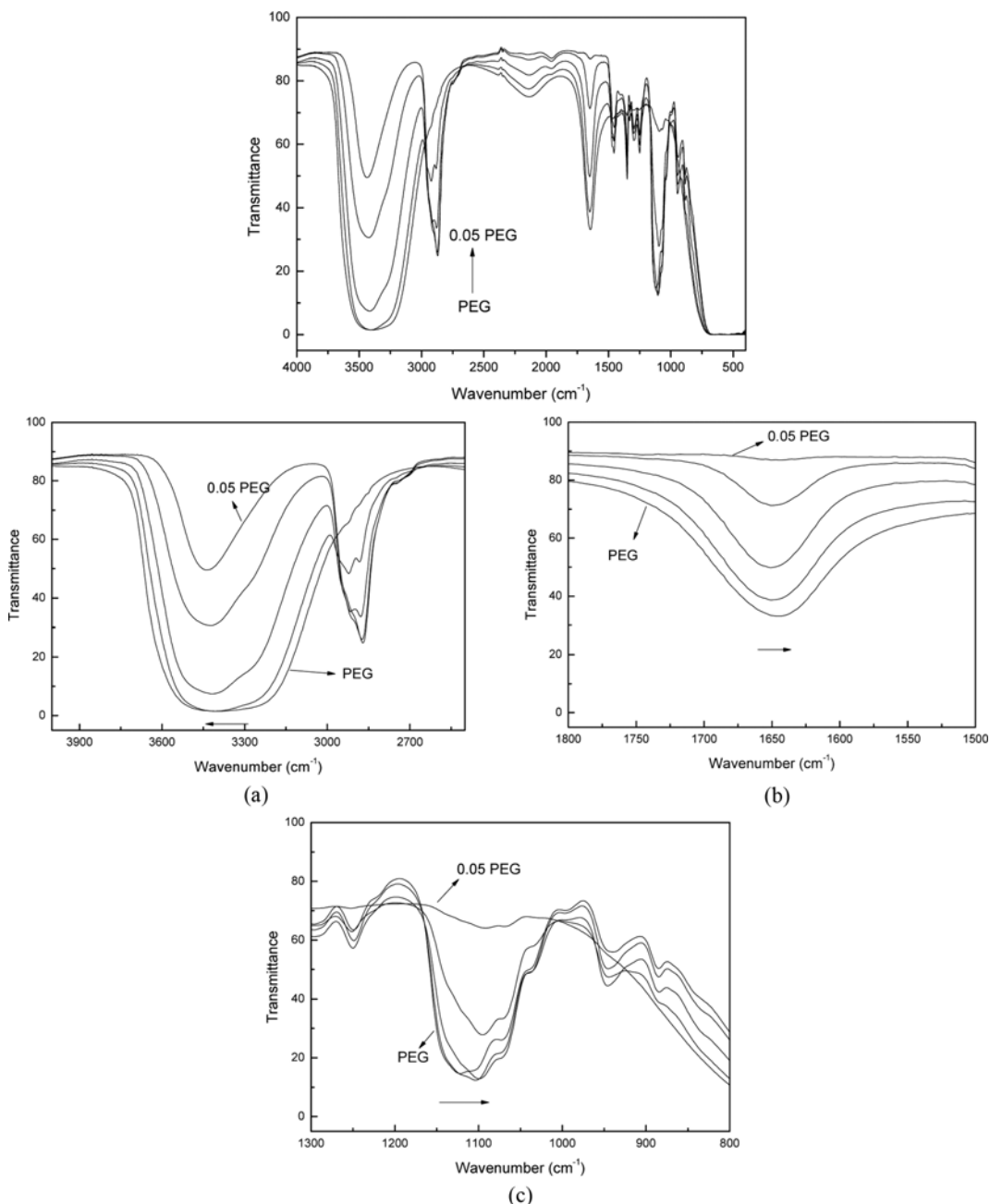


**Fig. 2. FTIR spectral changes of PEGW at various mass fractions with increasing H<sub>2</sub>O concentration: (a) 4,000-2,500 cm<sup>-1</sup>, (b) 1,800-1,500 cm<sup>-1</sup>, and (c) 1,300-800 cm<sup>-1</sup>. The changing trend was found with increasing H<sub>2</sub>O concentration.**

cally aligned interferometer, and is fitted with constringent BaF<sub>2</sub> pellets for the measurement of aqueous solution, an OPUS/IR operator, and IR source. A baseline correction was made for the spectra that were recorded in air; and then 15 mL solution was used on the FTIR spectrometer in every one of the measurements; the thin layer of samples are typically less than 2  $\mu\text{m}$  thickness. <sup>1</sup>H-NMR spectra were acquired using a Bruker ARX-400 nuclear magnetic resonance spectrometer and DMSO-d6 was used as an NMR solvent.

## RESULTS AND DISCUSSION

### 1. Spectral Properties of PEG+H<sub>2</sub>O

UV spectral changes of PEG+H<sub>2</sub>O are shown in Fig. 1.

Fig. 1 shows that the electronic transition band blue-shifts in the range of (190 to 250) nm with the increasing H<sub>2</sub>O concentration in PEGWs. The absorption band is assigned to the n $\rightarrow$ \* electronic transition of unshared electronic pair of hydroxyl oxygen atoms and ether oxygen atoms in PEG because the n $\rightarrow$ \* electronic transition of H<sub>2</sub>O is often found at the vacuum ultraviolet region. With the increasing H<sub>2</sub>O concentration, intermolecular hydrogen bonding of hydroxyl oxygen atoms and the ether oxygen atoms in PEG with hydrogen atoms in H<sub>2</sub>O happened easily. The results showed that PEG and H<sub>2</sub>O incurred intermolecular interaction and formed hydrogen-bonding as the formation of -CH<sub>2</sub>CH<sub>2</sub>OCH<sub>2</sub>CH<sub>2</sub>O(H) $\cdots$ HOH $\cdots$  and -CH<sub>2</sub>-CH<sub>2</sub>-O(CH<sub>2</sub>-CH<sub>2</sub>) $\cdots$ HOH $\cdots$ .

The FTIR spectral changes of PEG+H<sub>2</sub>O are shown in Fig. 2.

From Fig. 2, the fundamental stretching and deformation vibrations of water were present in the region of (3,700 to 3,000) cm<sup>-1</sup> and (1,700 to 1,600) cm<sup>-1</sup>, and the C-O-C asymmetry stretching vibrational band (Vas) of PEG was from 1,150 cm<sup>-1</sup> to 1,000 cm<sup>-1</sup>, so information about the interaction of PEG and H<sub>2</sub>O was obtained by detailed analysis of four parameters, such as peak position, intensity, bandwidth, and shape. From Fig. 2(a) the stretching vibrational band of hydroxyl in PEGW is found to shift toward higher frequency from 3,406 cm<sup>-1</sup> to 3,438 cm<sup>-1</sup> with increasing H<sub>2</sub>O concentration. The fact that the stretching vibrational band of hydroxyl in PEGW shifts toward higher frequency indicates that the interactions are due to the variational property of hydroxyl oxygen and ether oxygen in

PEG. From Fig. 1(b) the bending vibrational frequency of water changes from 1,651 cm<sup>-1</sup> to 1,643 cm<sup>-1</sup>, which has been reported to appear at 1,645 cm<sup>-1</sup> in water saturated low density polyethylene [27]. The fact that H-O-H bending vibrational band shifts towards lower frequency indicates that the interactions result from the variational property of hydrogen atom in H<sub>2</sub>O. Meanwhile, from Fig. 1(c) the stretching vibrational band of C-O-C in PEG shifts toward lower frequency from 1,106 cm<sup>-1</sup> to 1,092 cm<sup>-1</sup>, which indicates that interactions can be related to the variational property of oxygen atom in C-O-C in PEG. According to the above results, we present that the possible interactions between PEG and water result from the following two ways: (1) hydrogen bonding and interaction of hydrogen atom in H<sub>2</sub>O with hydroxyl oxygen atom in PEG by cross-linking as the formation of -CH<sub>2</sub>CH<sub>2</sub>O(H) $\cdots$ HOH $\cdots$ ; and (2) hydrogen bonding and interaction of hydrogen atom in H<sub>2</sub>O with ether oxygen atom in PEG as the formation of -CH<sub>2</sub>-CH<sub>2</sub>-O(CH<sub>2</sub>-CH<sub>2</sub>) $\cdots$ HOH $\cdots$ .

The present results show that the intermolecular hydrogen-bonding interaction in PEGW form as -CH<sub>2</sub>CH<sub>2</sub>OCH<sub>2</sub>CH<sub>2</sub>O(H) $\cdots$ HOH $\cdots$

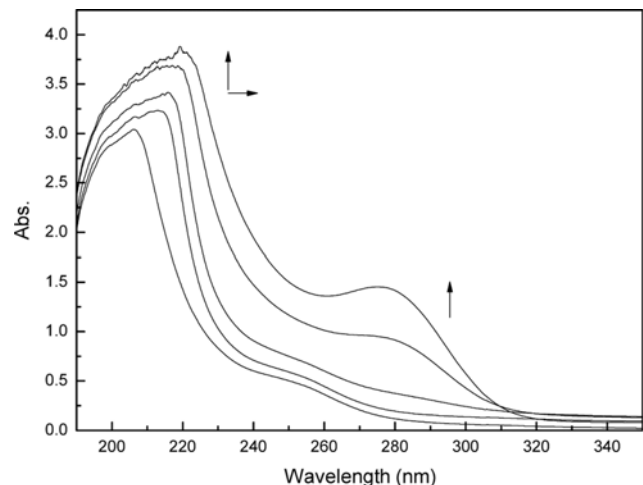


**Fig. 3. UV absorption spectral changes of PEG with the increasing SO<sub>2</sub> concentration.**

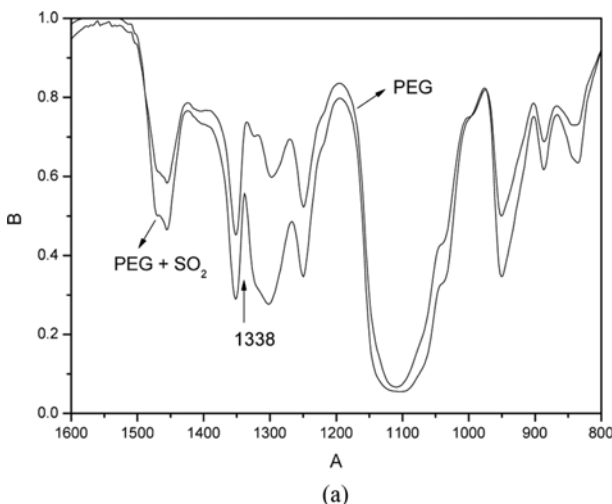
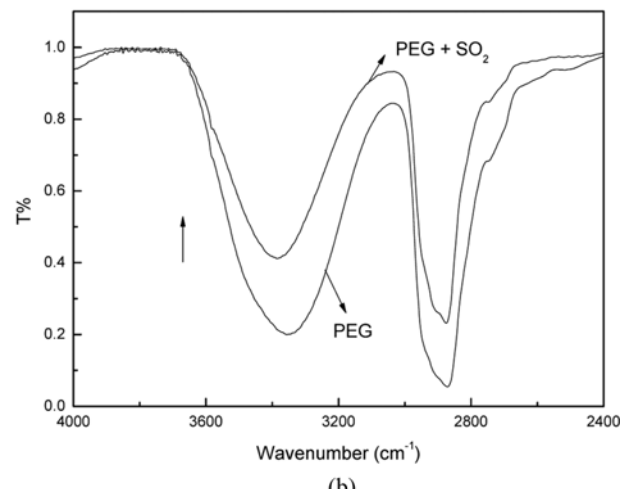


**Fig. 4. FTIR absorption spectra of PEG and PEG+SO<sub>2</sub>:** (a) 1,600-800 cm<sup>-1</sup>, (b) 4,000-2,400 cm<sup>-1</sup>.



and -CH<sub>2</sub>-CH<sub>2</sub>-O(CH<sub>2</sub>-CH<sub>2</sub>)<sub>n</sub>-HOH···.

## 2. Spectral Properties of PEG+SO<sub>2</sub>

In Fig. 3, the characteristic bands of PEG and SO<sub>2</sub> are respectively identified, but no information on a complexing reaction could be obtained. From the figure, the absorption band of n→π\* electron transition of oxygen atom in SO<sub>2</sub> ( $\Pi_3^4$ ) was observed at 278

nm and the absorption intensity of the band increases with increasing SO<sub>2</sub> concentration. Another absorption band, which was mainly due to π→π\* electron transition of sulfur atom in SO<sub>2</sub> ( $\Pi_3^4$ ) and n→σ\* electron transition of hydroxyl oxygen atom in PEG, shifts from 206 nm to 219 nm and the absorption intensity of the band increases. The shift results from the intermolecular hydrogen bond

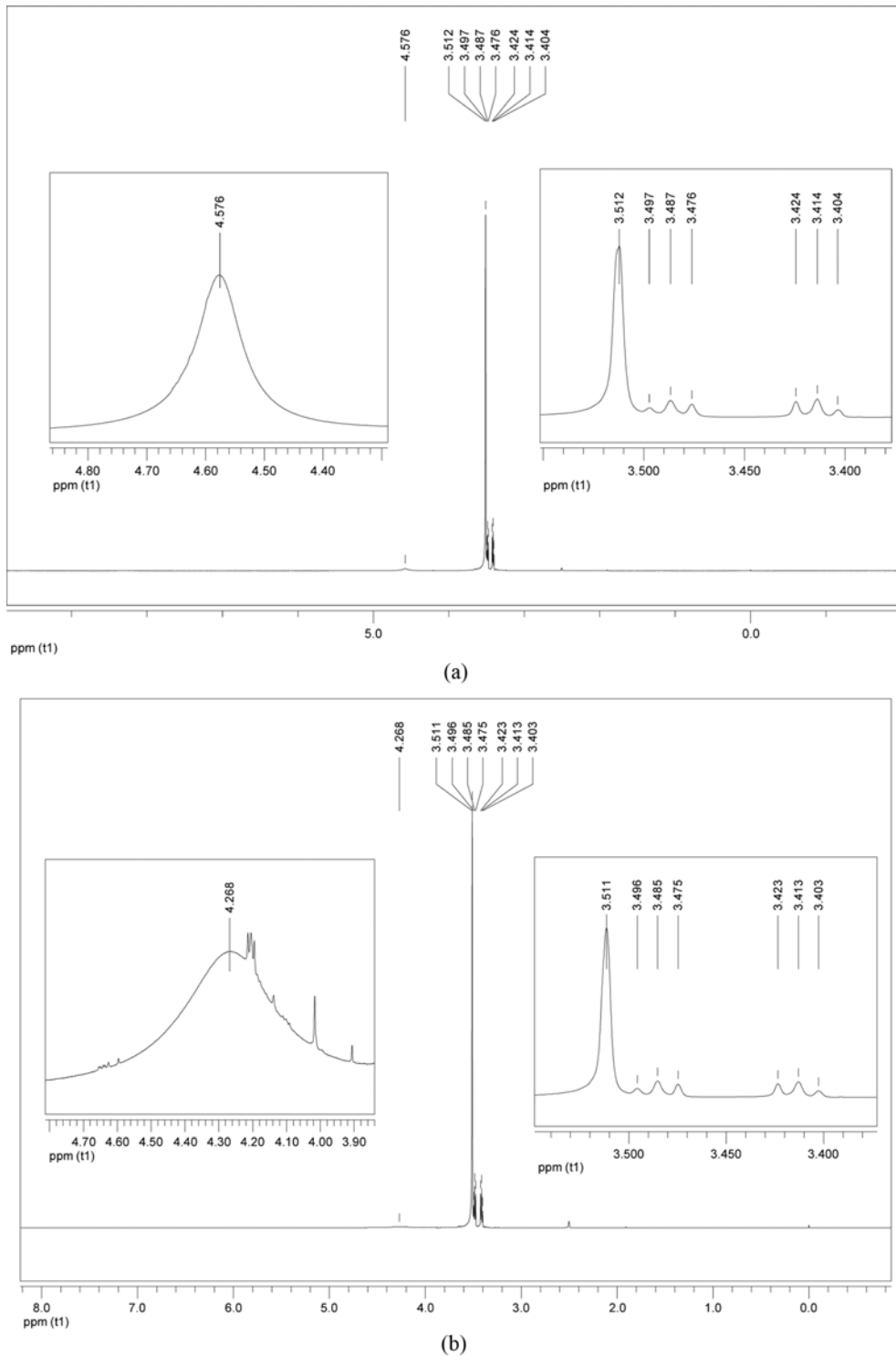


**Fig. 5.** <sup>1</sup>H-NMR spectral changes of PEG300 in the presence and absence of SO<sub>2</sub>. (a) <sup>1</sup>H-NMR spectrum of PEG, (b) <sup>1</sup>H-NMR spectrum of PEG300+SO<sub>2</sub>.

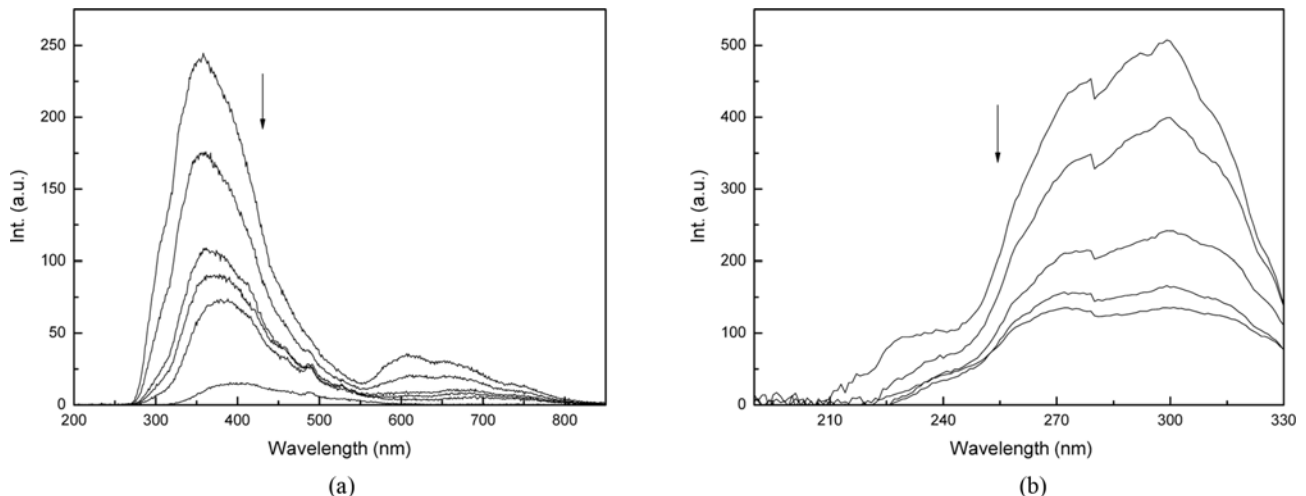


**Fig. 6. Fluorescence spectral change of PEG with the increasing  $\text{SO}_2$  concentration (a) excitation spectra and (b) emission spectra.**

of oxygen atoms in  $\text{SO}_2$  with hydroxyl hydrogen atoms in PEG and intermolecular  $\text{S}\cdots\text{O}$  interaction. The bonding of oxygen atoms of  $\text{SO}_2$  with hydroxyl hydrogen atoms of PEG results in the following results: (1) the decreasing effects of oxygen atoms on sulfur atom of  $\text{SO}_2$  make the  $\pi\rightarrow\pi^*$  electron transition of sulfur atom in  $\text{SO}_2$  change easier; and (2) the decreasing effects of hydroxyl hydrogen atoms on hydroxyl oxygen atoms in PEG make the  $n\rightarrow\sigma^*$  electron transition of hydroxyl oxygen atom in PEG also change easier.

The recorded FTIR spectra of PEG and PEG+ $\text{SO}_2$  are shown in Fig. 4.

In Fig. 4(a), an asymmetry stretching band ( $V_{\text{as}}$ ) of  $\text{SO}_2$  is observed at  $1,327 \text{ cm}^{-1}$ , and the C-O-C asymmetry stretching band at  $1,061 \text{ cm}^{-1}$  change is stronger, which shows that the C-O-C asymmetry stretching band of PEG is affected by  $\text{SO}_2$ . The absorption peak at  $1,327 \text{ cm}^{-1}$ , which is reported at  $1,344 \text{ cm}^{-1}$  for  $\text{SO}_2$  in non-complexing  $\text{CCl}_4$  [23], can be attributed to the  $V_{\text{as}}$  of  $\text{SO}_2$  because the IR and Raman spectra indicate the following values for the fundamental frequencies: symmetry stretching band ( $V_s$ )= $1,151.38 \text{ cm}^{-1}$ ,  $\delta=517.69 \text{ cm}^{-1}$ , and  $V_{\text{as}}=1,361.76 \text{ cm}^{-1}$ . Meanwhile, the phenomenon that the  $V_{\text{as}}$  of  $\text{SO}_2$  shifts towards lower wavenumber than  $V_{\text{as}}=1,361.76 \text{ cm}^{-1}$  can be due to the interaction of the sulfur atoms in  $\text{SO}_2$  with other atoms. The  $\text{SO}_2$  molecule is known to be polar and the sulfur atom to be electropositive; thus,  $\text{SO}_2$  behaves as an electron acceptor by the sulfur atom, and its interaction with hydroxyl oxygen atom (electronegative) in PEG should occur by the way of intermolecular  $\text{S}\cdots\text{O}$  interaction, which could not be discussed in the previous EGW+ $\text{SO}_2$  system [25] and PEGW+ $\text{SO}_2$  system [26].

However, the symmetry stretching band ( $V_{\text{as}}$ ) of  $\text{SO}_2$  at  $1,151 \text{ cm}^{-1}$  is strongly masked by the vibrations of PEG. In Fig. 4(b) a phenomenon is displayed. In the absence of  $\text{SO}_2$ , the stretching vibrational band of hydroxyl in PEG is observed at  $3,355 \text{ cm}^{-1}$ . In the presence of  $\text{SO}_2$ , the band is changed into a more peaked band at  $3,384 \text{ cm}^{-1}$ . The phenomenon could be due to the fact that the addition of  $\text{SO}_2$  affects the original hydrogen-bonding interaction among PEG molecules and forms new intermolecular hydrogen bonding of hydroxyl hydrogen atoms in PEG with oxygen atoms in  $\text{SO}_2$  and intermolecular  $\text{S}\cdots\text{O}$  interaction.

The  $^1\text{H-NMR}$  spectral results of PEG in the presence and absence

of  $\text{SO}_2$  are shown in Fig. 5.

Fig. 5(a) shows that the chemical shifts of hydrogen in  $-\text{CH}_2-$  appear at  $\delta=(3.404-3.512) \text{ ppm}$ , and the chemical shift of hydroxyl hydrogen appears at  $\delta=4.576 \text{ ppm}$  (2H) in the  $^1\text{H-NMR}$  spectrum of pure PEG. However, with increasing  $\text{SO}_2$  concentration in PEG, the bond length of O-H in EG molecules becomes longer and the electron cloud of hydroxyl hydrogen atoms in PEG molecules becomes thinner, so the signal changes into single peak and the chemical shift of hydrogen atoms in -OH groups shifts from  $\delta=4.576 \text{ ppm}$  to  $4.268 \text{ ppm}$  in DMSO (Fig. 5(a) and (b)). The phenomena can be due to the fact that the interaction of oxygen atoms in  $\text{SO}_2$  bonding with hydroxyl hydrogen atoms in PEG increases the shielding effect of hydroxyl hydrogen atoms in PEG, so that the signal changes into single peak and the signal of chemical shift of hydroxyl hydrogen in PEG moves towards a higher magnetic field.

Stable state fluorescence spectra with selective excitation of PEG with the increasing  $\text{SO}_2$  concentration were recorded and are shown in Fig. 6. Upon excitation at  $230 \text{ nm}$ , where the  $n\rightarrow\sigma^*$  electron transition of oxygen atom of PEG absorbs, strong fluorescence with emission positions at  $300-450 \text{ nm}$  and  $580-620 \text{ nm}$  are observed. The fluorescence intensity of the  $\sigma^*\rightarrow n$  electron transition of oxygen atom of PEG decreases with the increasing  $\text{SO}_2$  concentration. The phenomena can be due to the intermolecular interaction of the oxygen atom in PEG with  $\text{SO}_2$  as the formation of  $\text{S}\cdots\text{O}$  interaction.

According to the above IR, UV,  $^1\text{H-NMR}$ , and fluorescence spectral results, it is expected that PEG bonds with  $\text{SO}_2$  by the intermolecular hydrogen bonds of  $-\text{CH}_2\text{CH}_2\text{OH}\cdots\text{OSO}_2\cdots$  and intermolecular  $\text{S}\cdots\text{O}$  interaction.

### 3. Spectral Properties of PEGW+ $\text{SO}_2$

Fig. 7 shows the UV spectra of PEGW+ $\text{SO}_2$ , and the concentration of PEG was 0.10, 0.20, and 0.30 in mass fraction, respectively. All the three figures show a common phenomena that the absorption intensity of the band increases with the increasing  $\text{SO}_2$  concentration and the special absorption band red shifts. The absorption band observed around  $280 \text{ nm}$  was  $n\rightarrow\sigma^*$  electron transition of oxygen atom in  $\text{SO}_2$  and the band intensity increases with the increasing  $\text{SO}_2$  concentration. Meanwhile, the special absorption band present around  $200 \text{ nm}$  was found to red shift together with the in-

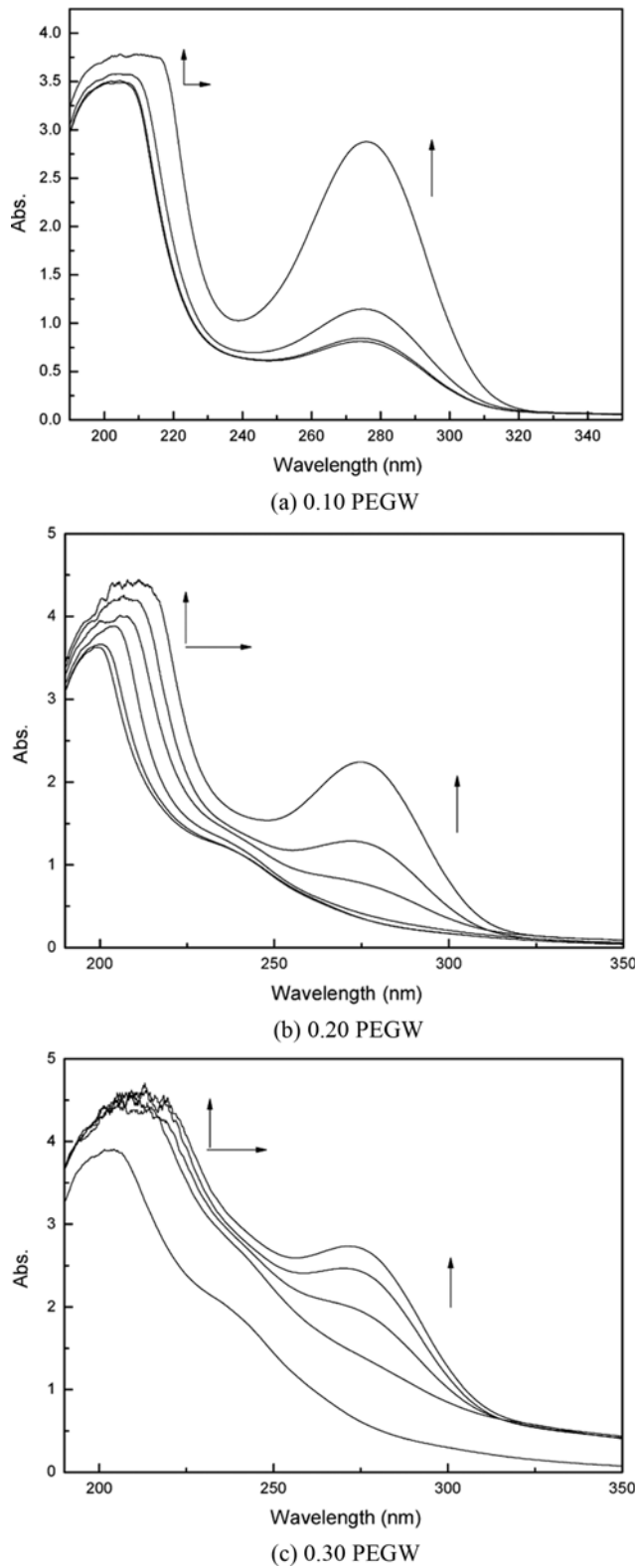


**Fig. 7. UV spectral changes of PEG in PEGW with the increasing SO<sub>2</sub> concentration.**

creasing absorption intensity. The results suggest the  $\pi \rightarrow \pi^*$  electron transition of SO<sub>2</sub> and  $n \rightarrow \sigma^*$  electron transition of oxygen atom of PEG in PEGW with the increasing SO<sub>2</sub> concentration.

The recorded FTIR spectra of H<sub>2</sub>O and H<sub>2</sub>O+SO<sub>2</sub> are shown in

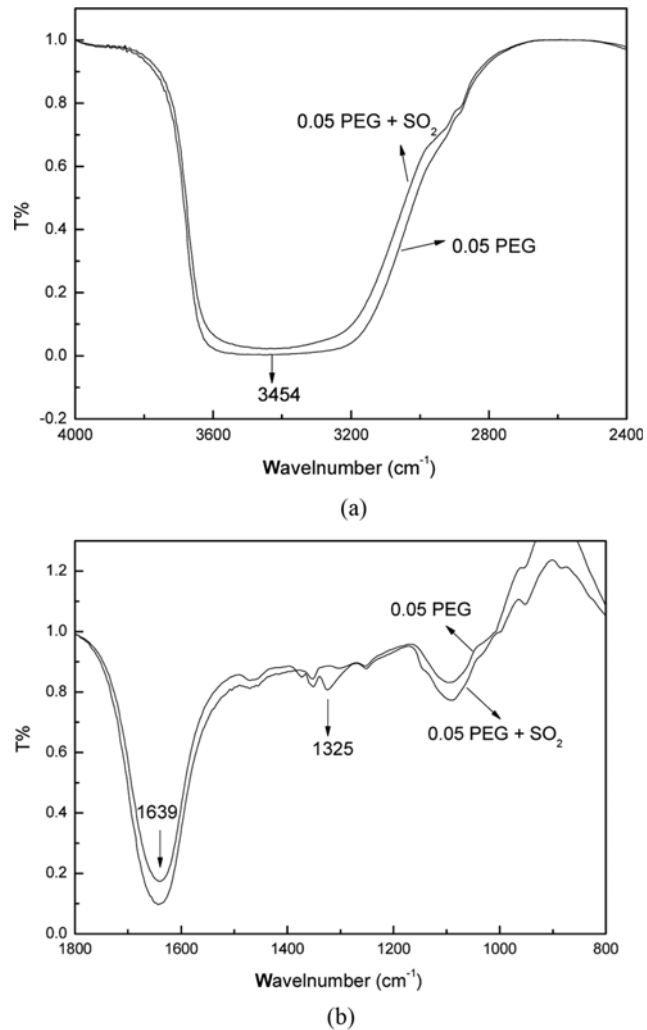


**Fig. 8. FTIR spectral changes of 0.05 PEG in mass fraction with the increasing SO<sub>2</sub> concentration. (a) 4,000-2,400 cm<sup>-1</sup>, and (b) 1,800-800 cm<sup>-1</sup>.**

the previous work [20]. From the spectra two special stretching bands are observed at 1,332 cm<sup>-1</sup> and 1,151 cm<sup>-1</sup>, which can be attributed to the Vas and Vs of SO<sub>2</sub> [21]. Fig. 8 is the FTIR spectra of PEGW+SO<sub>2</sub> with the concentration of PEG was 0.05 in mass fraction. In Fig. 8(a), the stretching vibrational band of hydroxyl in PEGW when  $w_1=0.05$  was observed at 3,444 cm<sup>-1</sup> and changed into a more peaked band and shifted toward lower frequency observed at 3,384 cm<sup>-1</sup> in the presence of SO<sub>2</sub>. This phenomenon can be explained by forming the new intermolecular hydrogen bonding. Together with Fig. 8(b), in which the stretching band was observed at 1,325 cm<sup>-1</sup>, and both the Vas and Vs of SO<sub>2</sub> shifts toward a lower wavenumber. This phenomenon was attributed to the interactions of PEG with SO<sub>2</sub> as the way of S···O.

Fluorescence spectra with selective excitation wavelength of PEGW with the increasing SO<sub>2</sub> concentration is shown in Fig. 9. Strong fluorescence emission peak are observed at the positions of 330-350 nm and 590-610 nm upon excitation wavelength at 205 nm. The fluorescence intensity of the  $\sigma^* \rightarrow n$  electron transition of oxygen atom of PEG in PEGW decreases with the increasing SO<sub>2</sub> concentration. The phenomena can be due to the intermolecular interaction

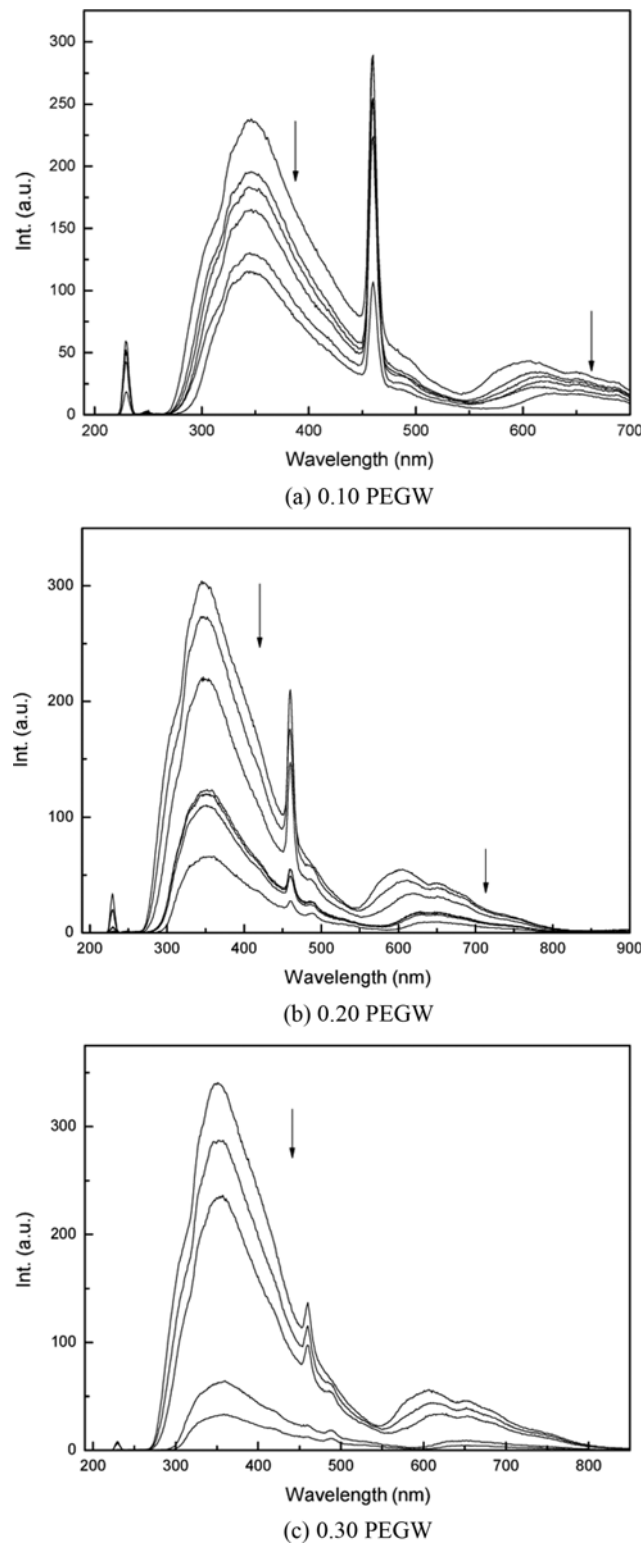


**Fig. 9. Fluorescence spectral changes of PEG in PEGW with the increasing  $\text{SO}_2$  concentration.**

of the oxygen atom in PEG with  $\text{SO}_2$  as the formation of  $\text{S}\cdots\text{O}$  interaction.

From the above discussion, conclusions can be drawn that the addition of  $\text{SO}_2$  affects the original hydrogen-bonding interaction among PEG molecules and forms the new intermolecular hydro-

gen bonding of hydroxyl hydrogen atom in PEG with oxygen atom in  $\text{SO}_2$  as the formation of  $-\text{CH}_2\text{CH}_2\text{OCH}_2\text{CH}_2\text{OH}\cdots\text{OSO}\cdots$ . Meanwhile, comparing the spectra of  $w_1=0.05$  PEGW+ $\text{SO}_2$  and PEG+ $\text{SO}_2$ , the constant H-O-H bending band in the absorption processes of  $\text{SO}_2$  is mainly due to the hydrogen interaction of PEG and  $\text{SO}_2$  rather than the reaction of water and  $\text{SO}_2$ .

## CONCLUSION

The pure PEG and its binary aqueous solutions (PEGW) present an optimized property for the absorption of  $\text{SO}_2$  because of its native hydrogen bonding sites for  $\text{SO}_2$ , so the absorption properties of  $\text{SO}_2$  can be related to hydrogen bonding and intermolecular  $\text{S}\cdots\text{O}$  interaction among molecules. The present results show that the possible interactions in PEGW result from the following two ways: (1) hydrogen bonding and interaction of hydrogen atom in  $\text{H}_2\text{O}$  with hydroxyl oxygen atom in PEG by cross-linking as the formation of  $-\text{CH}_2\text{CH}_2\text{O}-\text{CH}_2\text{CH}_2\text{O}(\text{H})\cdots\text{HOH}\cdots$ ; and (2) hydrogen bonding and interaction of hydrogen atom in  $\text{H}_2\text{O}$  with ether oxygen atom in PEG as the formation of  $-\text{CH}_2\text{CH}_2\text{O}(\text{CH}_2\text{CH}_2)\cdots\text{HOH}\cdots$ . In addition, the spectral analyses of added  $\text{SO}_2$  in pure PEG or  $w_1=0.05$  PEGW suggest that  $\text{SO}_2$  can interact with PEG by hydrogen bonds as the formation of  $-\text{OCH}_2\text{CH}_2\text{OCH}_2\text{CH}_2\text{OH}\cdots\text{OSO}\cdots$ , and intermolecular  $\text{S}\cdots\text{O}$  interaction of hydroxyl oxygen atom of PEG or ether oxygen atom in PEG with sulfur atom of  $\text{SO}_2$  as the formation of  $-\text{CH}_2\text{CH}_2\text{O}-\text{CH}_2\text{CH}_2\text{O}(\text{H})\cdots(\text{O})\text{SO}\cdots$  and  $-\text{CH}_2\text{CH}_2\text{O}-(\text{CH}_2\text{CH}_2\text{OH})\cdots(\text{O})\text{SO}\cdots$ .

## ACKNOWLEDGEMENTS

This work was supported by the National Natural Science Foundation of China (21166017), Program for New Century Excellent Talents in University (NCET-12-1017), the Research Fund for the Doctoral Program of Higher Education of China (20111514120002), the Natural Science Foundation of Inner Mongolia Autonomous Region (2011BS0601), Inner Mongolia Autonomous Region's Educational Commission (NJZZ11068), Program for Young Talents of Science and Technology in Universities of Inner Mongolia Autonomous Region (NJT-12-B13), the Inner Mongolia Talented People Development Fund, and Yongfeng Boyuan Industry Co., Ltd. (Jiangxi Province, China).

## REFERENCES

- M. J. Jin, Y. C. Hou, W. Z. Wu, S. H. Ren, S. D. Tian, L. Xiao and Z. G. Lei, *J. Phys. Chem. B*, **115**, 6585 (2011).
- R. K. Srivastava, W. Jozewicz and C. Singer, *Environ. Prog.*, **20**, 219 (2001).
- J. Werther, *J. Hazard. Mater.*, **144**, 604 (2007).
- I. Dahlan, K. T. Lee, A. H. Kamaruddin and A. R. Mohamed, *Environ. Sci. Technol.*, **40**, 6032 (2006).
- C. M. Wang, G. K. Cui, X. Y. Luo, Y. J. Xu, H. R. Li and S. Dai, *J. Am. Chem. Soc.*, **133**, 11916 (2011).
- Z. G. Sun, Y. Zhao, H. Y. Gao and G. X. Hu, *Energy Fuels*, **24**, 1013 (2010).
- K. Maneeintr, R. O. Idem, P. Tontiwachwuthikul and A. G. H. Wee, *Energy Procedia*, **1**, 1327 (2009).

8. C. N. Schubert, W. I. Echter, *The method of polymer ethylene glycol for removal of pollution from gases*, CN. Patent 1364096A (2002).
9. X. H. Wei, J. B. Zhang, P. Y. Zhang, L. W. Zhang, X. B. Li and M. J. Wan, *Removal of SO<sub>x</sub> from flue gas by ethylene glycol*, CN. Patent 101053746 (2007).
10. X. H. Wei, *Desulfurization & decarburization solution activities*, CN. Patent 02130605 (2002).
11. J. B. Zhang, P. Y. Zhang, G. H. Chen, F. Han and X. H. Wei, *J. Chem. Eng. Data*, **53**, 1479 (2008).
12. J. B. Zhang, P. Y. Zhang, F. Han, G. H. Chen, L. W. Zhang and X. H. Wei, *Ind. Eng. Chem. Res.*, **48**, 1287 (2009).
13. J. B. Zhang, F. Han, P. Y. Zhang, G. H. Chen and X. H. Wei, *J. Chem. Eng. Data*, **55**, 959 (2010).
14. J. B. Zhang, G. H. Chen, P. Y. Zhang, F. Han, J. F. Wang and X. H. Wei, *J. Chem. Eng. Data*, **55**, 1446 (2010).
15. J. B. Zhang, F. Han, X. H. Wei, L. K. Shui, H. Gong and P. Y. Zhang, *Ind. Eng. Chem. Res.*, **49**, 2025 (2010).
16. J. B. Zhang, J. B. Xiao, Y. X. Liu and X. H. Wei, *J. Chem. Eng. Data*, **55**, 5350 (2010).
17. J. B. Zhang, Q. Li, Z. H. Guo, K. X. Li, M. D. Xu, N. Zhang, T. Zhang and X. H. Wei, *Ind. Eng. Chem. Res.*, **50**, 674 (2011).
18. J. B. Zhang, L. H. Liu, T. R. Huo, Z. Y. Liu, T. Zhang and X. H. Wei, *J. Chem. Thermodyn.*, **43**, 1463 (2011).
19. N. Zhang, J. B. Zhang, Y. F. Zhang, J. Bai, T. R. Huo and X. H. Wei, *Fluid Phase Equilib.*, **313**, 7 (2012).
20. N. Zhang, J. B. Zhang and Y. F. Zhang, *Fluid Phase Equilib.*, **348**, 9 (2013).
21. P. Ivopoulos, M. Sotiropoulou, G. Bokias and G. Staikos, *Langmuir*, **22**, 9181 (2006).
22. D. P. Schofield, J. R. Lane and H. G. Kjaergaard, *J. Phys. Chem. A*, **111**, 567 (2007).
23. A. Lasgabaster, M. J. Abad, L. Barral and A. Ares, *Eur. Polym. J.*, **42**, 3121 (2006).
24. K. Dharmalingam and K. P. Ramachandran, *Physica B*, **4**, 1 (2006).
25. F. Palombo, M. Paolantoni, P. Sassi, A. Morresi and R. S. Cataliotti, *J. Mol. Liq.*, **125**, 139 (2006).
26. B. Yuan and X. M. Dou, *Spectrosc. Spectr. Anal. (In Chinese)*, **11**, 1319 (2004).
27. W. Wang, Y. Jin and Z. Su, *J. Phys. Chem. B*, **113**, 15742 (2009).